Connectivity Preserving Digitization of Blurred Binary Images in 2D and 3D

Peer Stelldinger [a] Ullrich Köthe [a]

[a] *Cognitive Systems Group, University of Hamburg, Vogt-Köln-Str. 30, D-22527 Hamburg, Germany*

Abstract

Connectivity and neighborhood are fundamental topological properties of objects in pictures. Since the input for any image analysis algorithm is a digital image, which does not need to have the same topological characteristics as the imaged real world, it is important to know, which shapes can be digitized without change of such topological properties. Most existing approaches do not take into account the unavoidable blurring in real image acquisition systems or use extremely simplified and thus unrealistic models of digitization with blurring. In some previous work we showed that certain shapes can be digitized topologically correctly with a square grid when some blurring with an arbitrary non-negative radially symmetric point spread function is involved. Now we extend this result to other common sampling grids in the two and even in the three dimensional space, including hexagonal, bcc and fcc grids.

Key words: r-regular shape, 3D digitization, topology preservation, point spread function, PSF

Introduction

A reliable image analysis algorithm requires a digital image having the properties of interest in common with its continuous preimage. There are several sampling theorems known, which describe under which circumstances certain topological properties (e.g. connectivity, neighborhood) of some shape do not change during digitization. These theorems mostly differ in the chosen digitization model and the used sampling grid. E.g. Pavlidis showed that so-called r-regular shapes can be digitized with square grids without any change in topology [4]. Serra proved the same for hexagonal grids [6] and we extended these results to arbitrary sampling grids [1]. All of these approaches used the subset digitization where a sampling point is set if and only if it lies within

the foreground region of the binary image, i.e. no blurring occurs. However, real optical systems blur the binary image before the light reaches the optical sensors. In addition to that each sensor integrates the intensity of light over some area. Both effects can be described as blurring – a convolution of the ideal binary image with a suitable point spread function. A binary image can be recovered by considering a particular level set $L_l = \{x \in \mathbb{R}^n | \hat{f}(x) \geq l\}$ of the blurred image $\hat{f}$, i.e. by thresholding. Of course the resulting shape heavily depends on the choice of the used point spread function. Latecki et al. [2,3] used a point spread function which is constant in its square-shaped support and proved that r-regular images can be topologically correctly reconstructed after blurring and sampling with a sufficiently dense square grid. In [1] we showed that this is also true for arbitrary 2D sampling grids when using a disc-shaped point spread function. Recently we proved that topology preservation in 2D can also be guaranteed for arbitrary non-negative radially symmetric point spread functions with bounded support [8], but this proof was restricted to square grids. In this paper we extend these results to other types of sampling grids, namely hexagonal and triangular grids and even three dimensional grids like cubic, bcc and fcc ones. Especially the 3D results are interesting since up to now only digitization without blurring has been investigated for higher dimensional grids [7].

1 Regular Sets, Sampling and Reconstruction

At first we define some basic mathematical concepts. The complement of a set A will be noted as A^c. The boundary ∂A is the set of all common accumulation points of A and A^c. A set A is open, if it does not intersect its boundary. Now let $n \in \{2, 3\}$ the dimension of the image. We denote the Euclidean distance between two points x, y as $d(x, y)$ and the Hausdorff distance between two sets A, B as $d_H(A, B) = \max\left(\max_{x \in A} \min_{y \in B} d(x, y), \max_{y \in B} \min_{x \in A} d(x, y)\right)$. $\mathcal{B}_r(c) := \{x \in \mathbb{R}^n | d(x, c) \leq r\}$ denotes the closed disc/ball and $\mathcal{B}_r^0(c) := (\mathcal{B}_r(c))^0$ denotes the open disc/ball of radius r and center c. The dilation of a set A with a disc/ball $\mathcal{B}_r$ is defined as $A \oplus \mathcal{B}_r := \{x \in \mathbb{R}^n | d_H(A, \{x\}) \leq r\}$ and the erosion is $A \ominus \mathcal{B}_r := \{x \in \mathbb{R}^n | d_H(A^c, \{x\}) > r\}$. $L_t(f)$ shall be the level set with threshold value t of an image function $f : \mathbb{R}^n \to \mathbb{R}$: $L_t(f) := \{x \in \mathbb{R}^n | f(x) \geq t\}$. $\mathbf{0}$ denotes the origin, e_x denotes the vector $(1|0)$, respectively $(1|0|0)$, and analogously e_y and e_z are defined.
Most of the existing topological sampling theorems require the binary images to be r-regular [1,2,3,6,7,8]. The concept of r-regular images was introduced independently by Serra [6] and Pavlidis [4]. These sets are extremely well behaved – they are smooth, round and do not have any cusps.

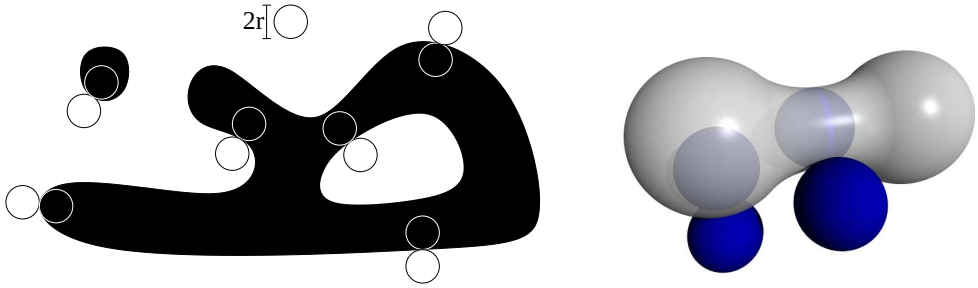

Figure 1. For each boundary point of a 2D/3D r-regular set there exists an outside and an inside osculating open disc/ball of radius r.

Definition 1 *A compact set $A \subset \mathbb{R}^n$ is called* r-regular *iff for each boundary point of A it is possible to find two osculating open discs/balls of radius r, one lying entirely in A and the other lying entirely in A^c (see Fig. 1).*

In order to compare analog with digital images, two things are needed: First a method to compare binary images and second a formal description of the processes of sampling and reconstruction. The method for comparison we choose is *weak r-similarity* (see [1,7]). If two sets are weakly r-similar, they are topologically equivalent (this criterion was chosen by Pavlidis [4]), have the same homotopy tree (as used by Serra [6]) and a Hausdorff distance of at most r. Note that topological equivalence and identity of homotopy trees are different criteria and neither implies the other (see [1]). In case of 3D digitization topological equivalence cannot generally be guaranteed (see [1]), thus we will then only use the bounded Hausdorff distance and the identity of the homotopy trees as similarity criterion. Unfortunately this covers much less information about topology than in 2D, as the example of two tori passing through each other vs. two separated tori illustrates (same homotopy tree in both cases).
The usefulness of a bounded Hausdorff distance as standalone similarity criterion is extensively discussed in the work of Ronse and Tajine (see [5] for a summary). The generality of their approach is remarkable, but it cannot directly be used for our problem, since it does not say anything about the topology of a digital reconstruction and it cannot be applied to images which are blurred by some point spread function.

Definition 2 *Two bounded sets $A, B \subset \mathbb{R}^n$ are called* weakly r-similar *if there exists a homeomorphism $f : \mathbb{R}^n \to \mathbb{R}^n$ such that $x \in A \Leftrightarrow f(x) \in B$, and the Hausdorff distance between the set boundaries $d_H(\partial A, \partial B) \leq r \in \mathbb{R}_+ \cup \{\infty\}$. The used homeomorphism is called* $\mathbb{R}^n$-homeomorphism *between A and B.*

The following definition captures the 2D and 3D case of digitization. The differences from 3D to 2D are written in brackets.

Definition 3 *A countable set $S \subset \mathbb{R}^n$ of* sampling points *with $d_H(\mathbb{R}^n, S) \leq r'$ for some $r' \in \mathbb{R}_+$ such that $S \cap A$ is finite for each bounded set A, is called* r'-grid. *r' is called the covering radius. The* pixel (voxel) $\mathrm{Pixel}_S(s)$ *(*$\mathrm{Voxel}_S(s)$*) of a sampling point s is its Voronoi region, i.e. the set of all points lying at least as near to this point as to any other sampling point.*
Given a translation vector t and a rotation matrix R in 2D, a square r'-grid *is defined by $t + r'S \cdot R$ with $S := \sqrt{2}\mathbb{Z}^2$. Equivalently* hexagonal *and* triangular r'-grids *are defined by $S := \{(\frac{\sqrt{3}}{2}x_1, \frac{3}{2}x_2) | x_1, x_2 \in \mathbb{Z}, x_1 + x_2 \equiv 0(\mathrm{mod}2)\}$ and $S := \{(\frac{\sqrt{3}}{2}x_1, 2x_2), (\frac{\sqrt{3}}{2}x_1, 2x_2+1) | x_1, x_2 \in \mathbb{Z}, x_1+x_2 \equiv 0(\mathrm{mod}2)\}$, respectively. In 3D* cubic r'-grids *are defined by $t+r'S\cdot R$ with a 3D translation vector t and a 3D rotation matrix R and with $S := \sqrt{3}\mathbb{Z}^2$. Equivalently* bcc *and* fcc r'-grids *are defined by $S := \{\frac{2}{\sqrt{5}}(x_1, x_2, x_3) | x_1, x_2, x_3 \in \mathbb{Z}, x_1 \equiv x_2 \equiv x_3(\mathrm{mod}2)\}$ and $S := \{(x_1, x_2, x_3) | x_1, x_2, x_3 \in \mathbb{Z}, x_1 + x_2 + x_3 \equiv 0(\mathrm{mod}2)\}$. All these grids are scaled such that they are r'-grids.*
The intersection of $A \subseteq \mathbb{R}^n$ with S is called the S-digitization of A, *and the restriction of the domain of A's characteristic function to S is the associated* digital binary image *The* S-reconstruction *is the union of all pixels belonging to the sampling points in the S-digitization. Two pixels (voxels) are* adjacent *if they share an edge (face). Two pixels (voxels) of $\hat{A}$ are* connected *if there exists a chain of adjacent pixels (voxels) in $\hat{A}$ between them. Two sampling points are adjacent (connected) if their pixels (voxels) are adjacent (connected). A* component *of $\hat{A}$ is a maximal set of connected pixels (voxels).*

The most obvious approach for sampling is to restrict the domain of the image function to the sampling grid. But this ideal digitization does not take into account any blurring. This can be added by a convolution of the image with some point spread function before sampling. Digitization of a binary image has three steps: At first the image gets blurred due to the camera optic. Then the blurred grayscale preimage gets sampled and reconstructed (To reconstruct a grayscale image means to fill each pixel with the image value at the corresponding sampling point). Finally the image gets thresholded in order to get a binary result. Mathematically the last two steps commute. Thus the definition of a digitization without blurring completely determines how to digitize with some blurring: You simply have to blur the original set, apply a threshold function and digitize the result.

Definition 4 *A function $k : \mathbb{R}^2 \longrightarrow \mathbb{R}$ is called a* p-point spread function (p-PSF) *if (1) $\int_{\mathbb{R}^2} k(x)dx = 1$, (2) k is nonnegative, (3) k is radially symmetric, (4) k has compact support of radius of at most p. Now let $A \subset \mathbb{R}^2$ be a binary set. Then its characteristic function $\chi_A : \mathbb{R}^2 \to \{0, 1\}$ is 1 for any $x \in A$ and 0 for any $x \notin A$. Given a p-PSF k, the* blurred image of A by using k *is defined as $f_A := k \star \chi_A$ ($\star$ denotes convolution).*

Based on these definitions we are able to prove a sampling theorem for blurred binary images.

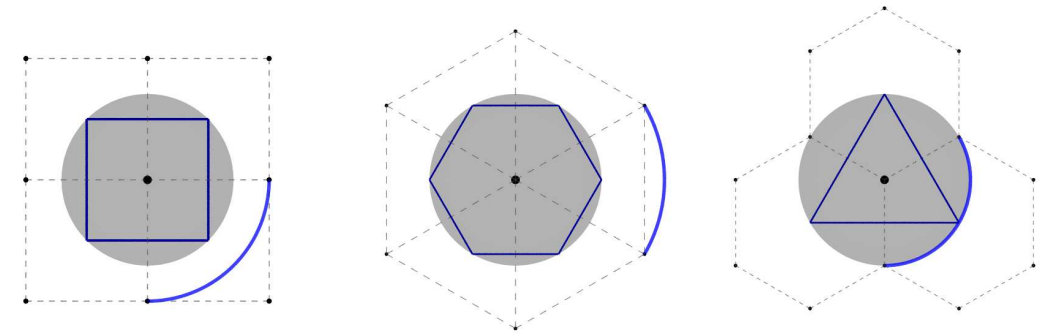

(a) square grid (b) hexagonal grid (c) triangular grid

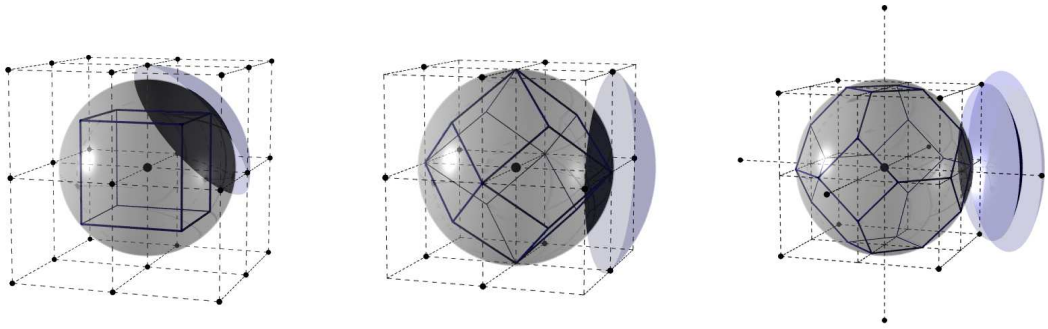

(d) cubic grid (e) fcc grid (f) bcc grid

Figure 2. Different grids with identical covering radius r'. Pixels/Voxels are marked by solid lines. the dashed lines connect adjacent sampling points in (a) to (c). In (d) to (f) the dashed lines illustrate the embedding into a cubic grid. The circle segments in (a) to (c) and the spherical caps in (d) to (f) always contain at least one adjacent sampling point, regardless of the rotation of the grid around the central sampling point. In order to deal with the two ypes of adjacent sampling points in the bcc-grid (f), there are two spherical caps with different radii necessary.

2 Sampling-Theorem for Blurred Binary Images

In a previous paper we already proved a sampling theorem for non-blurred binary images and a theorem for binary images after blurring with a constant disc-shaped PSF [1]:

Theorem 5 *Let $r \in \mathbb{R}_+$ and A a 2D r-regular set. Then A is weakly r'-similar to any S-reconstruction with some r'-grid S, $0 < r' < r$.*

Theorem 6 *Let $r, r', p \in \mathbb{R}_+$ be positive numbers with $r' + p < r$ and let A be a 2D r-regular set, k_p a disc-shaped PSF being constant in its support of radius p, and $f_A = k_p \star \chi_A$ the blurred image of A. Further let L_l be the level´set of f_A with some level l and let S be an arbitrary r'-grid. Then the S-reconstruction $\hat{L}_l$ of L_l is weakly $(r' + p)$-similar to A.*

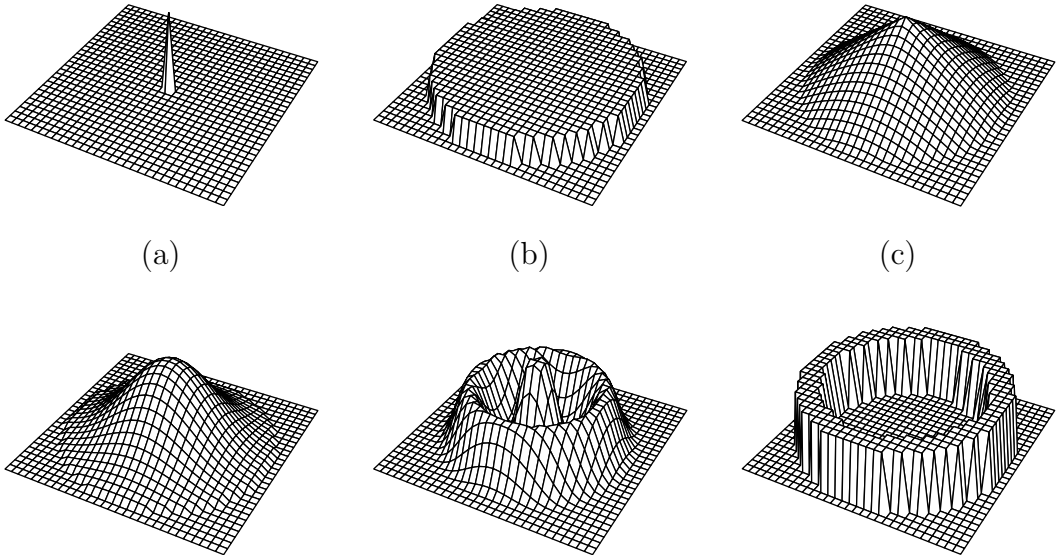

Figure 3. The definition of p-PSFs is very broad. 2D Examples are the dirac impulse (a), which leads to a non-blurred digitization, the disc-PSF (b) as used in [1,7], conic PSFs (c), truncated Gaussians (d), and even non-descending PSFs (e) and (f). While (f) is an artificial example showing what kind of PSF is also allowed, (e) is of practical interest, since the camera aperture can cause such diffraction patterns.

In [8] we generalized these results to other types of point spread functions by restricting ourselves to square grids. We showed that any p-PSF with $p < r'$ can be used for digitization with an r'-square grid, such that any r-regular set ($r > r' + p$) is topologically equivalent to its digital reconstruction:

Theorem 7 *Let $r, r', p \in \mathbb{R}_+$ be positive numbers with $p < r'$ and $r' + p < r$ and let A be a 2D r-regular set, k_p an arbitrary p-PSF, and $f_A = k_p \star \chi_A$ the blurred image of A. Further let L_l be the level set of f_A with some level l and let S be a square r'-grid. Then the S-reconstruction $\hat{L}_l$ of L_l is weakly $(r' + p)$-similar to A.*

In this paper we refine the proof methods and are thus able to generalize the results to other sampling grids, namely hexagonal and triangular grids and even to the three-dimensional cubic, bcc and fcc grids. In case of higher dimensions we had up to now only been able to regard digitization without blurring (see [7]):

Theorem 8 *Let $r \in \mathbb{R}_+$ and $A \subset \mathbb{R}^n$ an r-regular set. Further let $\hat{A}$ be the reconstruction of A with an arbitrary r'-grid S in $\mathbb{R}^n$, $0 < r' < r$. Then A and $\hat{A}$ have identical homotopy trees and the Hausdorff distance between their boundaries is at most r'.*

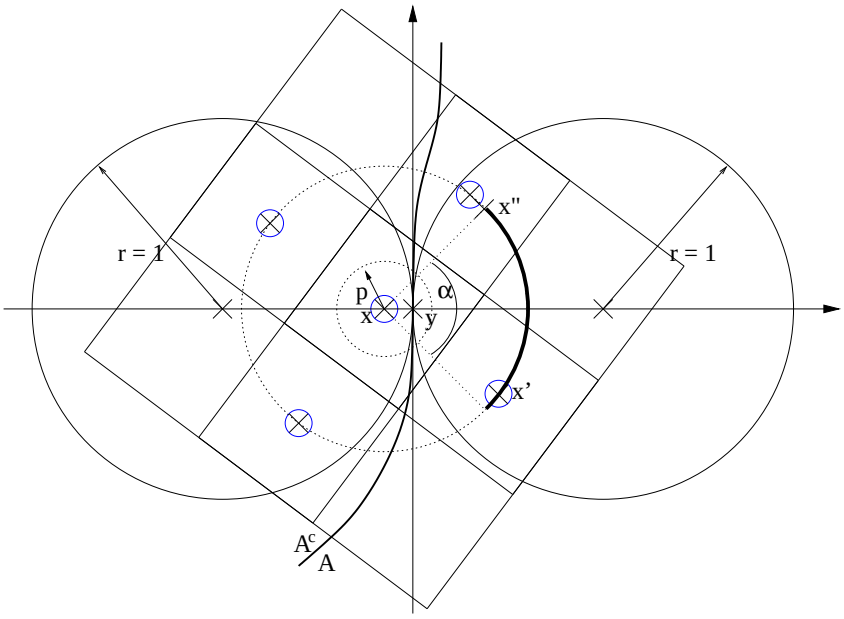

Figure 4. Illustration of the 2D case: At least one of the sampling points being adjacent to x lies in the bold sector of the circle. The sampling points are marked with blue circles.

Now we are able to reunite these ways, in order to get a sampling theorem dealing with arbitrarily blurred binary images in 2D and 3D.

Theorem 9 *Let S be a square, hexagonal, trigonal, cubic, bcc or fcc r'-grid in 2D respectively 3D. Now let A be an r-regular set and k_p be an arbitrary p-PSF in the given dimension. Further let L_l be the level set of f_A with some level l. Then the S-reconstruction $\hat{L}_l$ of L_l has the same homotopy tree as A and the Hausdorff distance between their boundaries is at most $r'+p$ (in the 2D case A and $\hat{L}_l$ are even weakly $(r'+p)$-similar) if the following inequations are true:*

S	*inequations*		
square grid	$p < 1.1651r'$	,	$r'+p<r$
hexagonal grid	$p < 1.80191r'$	,	$r'+p<r$
triangular grid	$p < 0.480269r'$	,	$r'+p<r$
cubic grid	$p < 0.716879r'$	,	$r'+p<r$
bcc grid	$p < 1.59677r'$	,	$1.10848r'+p<r$
fcc grid	$p < 1.1651r'$	,	$r'+p<r$

PROOF. Due to the support of the PSF, $f_A(x)=1$ for any $x \in A \ominus \mathcal{B}_p$ and analogously $f_A(x)=0$ for any $x \notin A \oplus \mathcal{B}_p$. Due to r-regularity of A, the sets

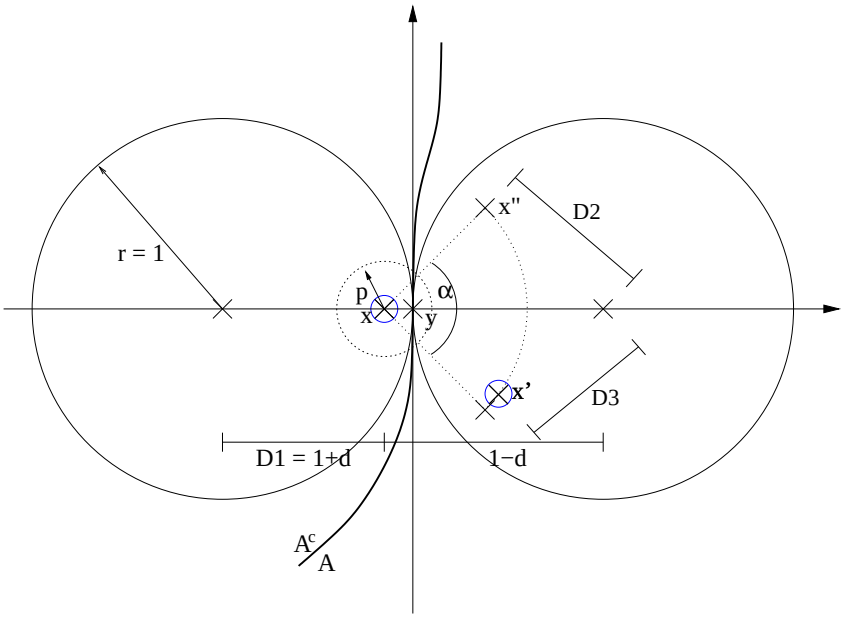

Figure 5. Illustration of the 2D case: The distance D_3 between the center of the inside osculating disc and the adjacent sampling point x' is at most equal to the distance D_2.

$B := A \ominus \mathcal{B}_p$ and $C := A \oplus \mathcal{B}_p$ are both $(r-p)$-regular and weakly p-similar to A. Due to Theorem 5 their S-reconstructions $\hat{A}, \hat{B}$ are weakly $(r'+p)$-similar to A in the 2D case and due to theorem 8 $\hat{A}$ and $\hat{B}$ have the same homotopy tree as A and the Hausdorff distance to A is at most $r'+p$ in both cases. Obviously $\hat{B} \subseteq \hat{L}_l \subseteq \hat{C}$, which implies that the Hausdorff distance between ∂A and $\partial \hat{L}_l$ is bounded by $r'+p$. Thus in 3D we only have to show that L_l has the same homotopy tree as A, which is true if any sampling point $x \in \hat{L}_l$ is (directly) connected in $\hat{L}_l$ with some sampling point $y \in \hat{B}$ and if any sampling point $x \notin \hat{L}_l$ is connected in $\hat{L}_l^c$ with some sampling point $y \notin \hat{C}$. This is also all we have to show in the 2D case since then no additional component or hole can occur and thus L_l is $\mathbb{R}^2$-homeomorphic to A.
Thus both in 2D and in 3D it is sufficient to prove that for any $x \in S$ with $f_A(x) \in (0,1)$ there exists an adjacent sampling point $x_{\geq}$ with $f_A(x_{\geq}) \geq f_A(x)$ and an adjacent sampling point $x_{\leq}$ with $f_A(x_{\leq}) \leq f_A(x)$.
Let $x \in S$ be a sampling point with $f_A(x) \in (0,1)$ and let $y \in \partial A$ be the boundary point of A being nearest to x. Due to r-regularity there exists a unique nearest boundary point. Without loss of generality let $x = d \cdot e_x$ (note that $-p < d < p$ and thus d can be negative as shown in the example of Fig. 4 and 5), $y = \mathbf{0}$, $r = 1$ (any other case can be derived by choosing an appropriate scale and coordinate system) and let $\mathcal{B}_1^0(e_x)$ be the inside and $\mathcal{B}_1^0(-e_x)$ be the outside osculating r-disc/r-ball of A in y (see Fig. 4). Then every sampling point being adjacent to x lies on the circle/sphere with some radius R and center x (see the following table for the values of R regarding to the chosen sampling grid; in case of a bcc grid two different radii have to be considered,

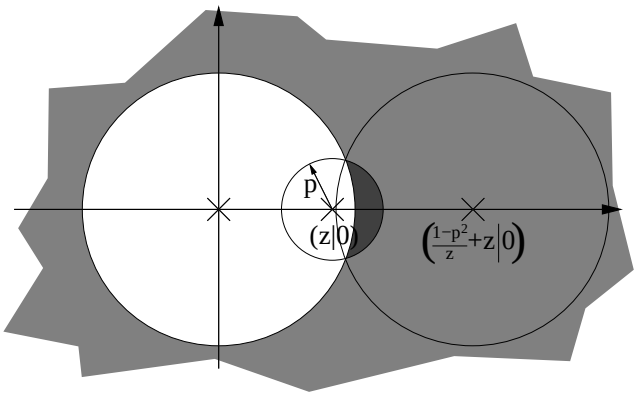

Figure 6. The helper function h describes the result of blurring the complement of the unit disc/ball image with the PSF at some position with distance z to the origin.

since there are two types of adjacent sampling points). Now for each sampling grid there exists a minimal angle α such that the sector/spherical cap of angle α has to contain at least one sampling point x' on the circle/sphere.

S	R	α
square grid	$\sqrt{2}r'$	$90°$
hexagonal grid	$\sqrt{3}r'$	$60°$
triangular grid	$1r'$	$120°$
cubic grid	$\frac{2}{\sqrt{3}}r'$	$2\cos^{-1}(\frac{1}{\sqrt{3}}) \approx 109.5°$
bcc grid	$2\sqrt{\frac{4}{5}}r', 2\sqrt{\frac{3}{5}}r'$	$2\cos^{-1}\left(\frac{1}{\sqrt{5-2\sqrt{3}}}\right) \approx 72.4°$
fcc grid	$\sqrt{2}r'$	$90°$

Let x'' be one point on the sector/spherical cap boundary (in 2D there are exactly two such points) (see Fig. 4). Now let $D_1 = 1 + d$ be the distance between $(-1|0)$ and x, let $D_2 = \sqrt{R^2 + (1-d)^2 - 2R(1-d)\cos\frac{\alpha}{2}}$ be the distance between $(1|0)$and x'' and let D_3 be the distance between $(1|0)$ and x' (see Fig. 5), then obviously $D3 \leq D_2$.

Now let $B := \mathcal{B}_1^c$ be a binary image, which is the complement of the unit disc/ball. By using B we construct a helper function $h : [1-p, 1+p] \longrightarrow [0, 1]$ with $h(z) := f_B((z|0))$ (see Fig. 6 for an illustration of the 2D case). Obviously h is monotonically increasing since the non-zero area $\mathcal{B}_p(z_1 e_x) \cap B$ of the image B covered by the PSF at postion $z_1 e_x$ is a translated superset of the same area $\mathcal{B}_p(z_2 e_x) \cap B$ at position $z_2 e_x$ for any $z_1, z_2 \in [1-p, 1+p]$ with $z_1 > z_2$. Now consider the intersection points of the circles/spheres $\partial\mathcal{B}_1$ and $\partial\mathcal{B}_p(z e_x)$. There exists exactly one other circle/sphere of radius 1 sharing these points. This circle/sphere is centered in $(\frac{1-p^2}{z}+z)e_x$. As Fig. 6 illustrates,

$1 - h(z) \geq h(\frac{1-p^2}{z})$.
Since the outside osculating disc/ball $\mathcal{B}_1(-e_x)$ is a subset of A^c (see Fig. 4), $f_A(x)$ is at most equal to $h(D_1)$. Analogously since the inside osculating disc/ball $\mathcal{B}_1(e_x)$ is a subset of A, $f_A(x')$ is at least equal to $1 - h(D_3)$. With $D_3 \leq D_2$ it follows that $1 - h(D_2) \leq 1 - h(D_3)$. Thus we only have to show that $h(D_1) \leq 1 - h(D_2)$ in order to prove $f_A(x) \leq f_A(x')$.
Now if we can show that $h(D_1) > h(\frac{1-p^2}{D_2})$ is true for the allowed values of R, p and α, we are finished since this implies $h(D_1) > 1 - h(D_2)$. Due to monotony of h, the inequation $h(D_1) > h(\frac{1-p^2}{D_2})$ is equivalent to $D_1 > \frac{1-p^2}{D_2} > \frac{1-(1-r')^2}{D_2}$, which is equivalent to $D_2^2 D_1^2 - (1-p^2)^2 > 0$. By substitution of D_1 and D_2 we get

$$g(d, R, \alpha, p) := (R^2(1-d)^2 - 2R(1-d)\cos\frac{\alpha}{2})(1+d)^2 - (1-p^2)^2 > 0.$$

In order to determine the minimal values of g regarding d, we compute the zeros of the derivative $\frac{\mathrm{d}g}{\mathrm{d}d}$: These are

$$d_0 = -1$$

and

$$d_{1,2} = \frac{1}{4}\left(2 - 3R\cos\frac{\alpha}{2} \overset{+}{-} \sqrt{4 - 4R\cos\frac{\alpha}{2} - 8R^2 + \left(3R\cos\frac{\alpha}{2}\right)^2}\right).$$

Since $-p < d < p$ the minimal value of g for different d must be achieved with $d \in \{-p, p, d_1, d_2\}$.
Thus we get four inequations which all have to be true:

$$g(-p, R, \alpha, p) > 0,$$

$$g(p, R, \alpha, p) > 0,$$
$$g(d_1, R, \alpha, p) > 0$$

and

$$g(d_2, R, \alpha, p) > 0.$$

Fig. 7 shows the zero crossings of these inequations for the different sampling grids as functions of p over r' with all inequations being true inside the hatched area. One can see that the upper bound of this area is given by two zero level lines of different functions, one of them being linear. As can be seen in Fig. 7, the triangle between their intersection point, the origin, and the intersection point of the linear function and the x-axis lies completely inside the hatched area. This triangle is exactly the one described by the inequations in theorem 9. It follows that for p and r' inside the triangle and for any $x \in S$ with $f_A(x) \in (0, 1)$ there exists an adjacent sampling point $x_{\geq}$ with $f_A(x_{\geq}) \geq f_A(x)$ and analogously there exists an adjacent sampling point $x_{\leq}$ with $f_A(x_{\leq}) \leq f_A(x)$. $\square$

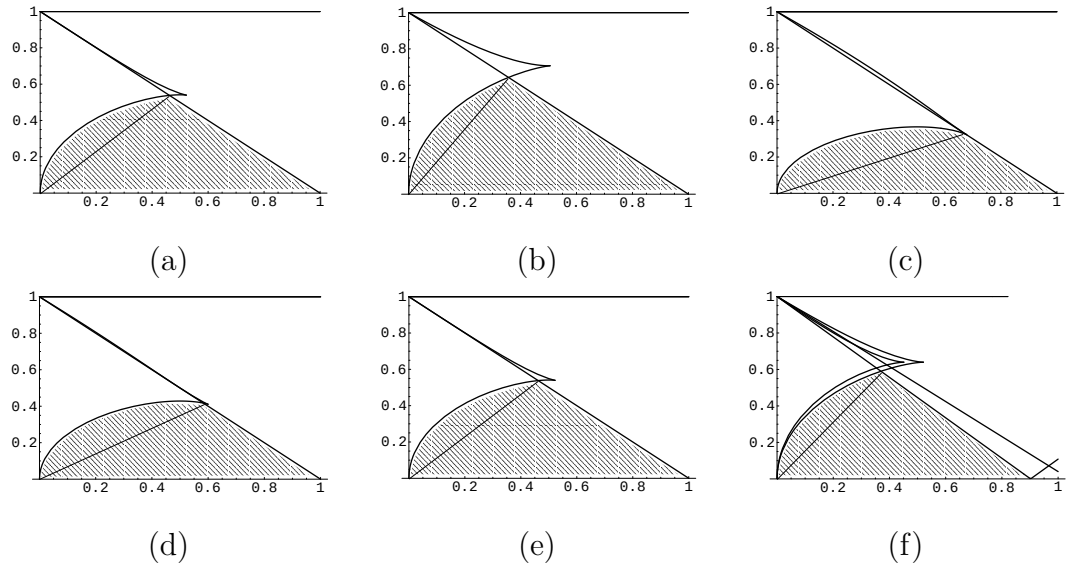

Figure 7. The hatched area shows the allowed pairs of values of $\frac{r'}{r}$ (x-axis) and $\frac{p}{r}$ (y-axis) for the different sampling grids ((a) square, (b) hexagonal, (c) triangular, (d) cubic, (e) fcc, (f) bcc). The solid lines are the zero crossings of the inequations as described in the text. (f): Since there are two different types of adjacency in the bcc grid, the number of inequations which have to be fulfilled is twice as big as in the other cases. The triangles inside the hatched areas are given by the inequations of theorem 9. They give an approximation of the allowed area which is simple to use.

Since the class of possible point spread functions is very general, this sampling theorem can be applied to much more practical applications than the previous ones.

3 Conclusions

We proved a sampling theorem which can be summarized in an extremely simple statement: By using an arbitrary p-PSF and a square, hexagonal, triangular, cubic, bcc or fcc r'-grid, we can digitize any r-regular binary image without any change in the homotopy tree if only r', p and r fulfill two simple linear inequations which only depend on the chosen sampling grid. This is true for any threshold value used for binarization.
Realistic cameras have very complicated point spread functions and often one does not know the exact PSF. Due to our result one does not have to know this, if only one can assume that it is nonnegative, radially symmetric and has a bounded support of known (or estimated) radius. Thus our result can be applied to real camera acquisition systems much better than previous findings. One can also see that the best choice of some sampling grid in 2D is a hexagonal grid since this grid has the biggest area of allowed values of p and

r' relatively to some regularity measure r. In three dimensions the fcc and bcc grids are better than the cubic grid. While using an fcc grid allows higher values of r' for small p, the bcc grid is better when having high values of p and small values of r'.

References

[1] Köthe, U., Stelldinger, P.: *Shape Preserving Digitization of Ideal and Blurred Binary Shapes*. In: I. Nyström et al. (Eds.): DGCI 2003, LNCS **2886**, pp. 82-91, Springer, 2003.

[2] Latecki, L.J., Conrad, C., Gross, A.: *Preserving Topology by a Digitization Process*. Journal of Mathematical Imaging and Vision **8**, pp. 131–159, 1998.

[3] Latecki, L.J.: *Discrete Representation of Spatial Objects in Computer Vision*. Kluwer, 1998.

[4] Pavlidis, T.: *Algorithms for Graphics and Image Processing*. Computer Science Press, 1982.

[5] Ronse, C., Tahine, M.: *Morphological Sampling of Closed Sets*. Image Analysis and Stereology **23**, pp. 89–109, 2004.

[6] Serra, J.: *Image Analysis and Mathematical Morphology*. Academic Press, 1982.

[7] Stelldinger, P., Köthe U.: *Towards a General Sampling Theory for Shape Preservation*. In: Image and Vision Computing, Special Issue on Discrete Geometry for Computer Vision **23**, Issue 2, pp. 237–248, Elsevier, 2005.

[8] Stelldinger, P., Köthe U.: *Shape Preserving Digitization of Binary Images after Blurring*. In: E. Andres et al. (Eds.): DGCI 2005, LNCS **3429**, pp. 383–391, Springer, 2005.